Proc. Natl. Acad. Sci. USA
Vol. 93, pp. 1982–1987, March 1996
Biochemistry

A general two-process model describes the hydrogen exchange behavior of RNase A in unfolding conditions

(two-process model/unfolding intermediates/exchange pathway)

STEWART N. LOH*, CAROL A. ROHL*, THOMAS KIEFHABER†, AND ROBERT L. BALDWIN*

*Department of Biochemistry, Stanford Medical Center, Stanford, CA 94305-5307; and †Abteilung Biophysikalische Chemie, Biozentrum der Universität, Klingelbergstrasse 70, CH-4056, Basel, Switzerland

Contributed by Robert L. Baldwin, November 13, 1995

ABSTRACT **When NMR hydrogen exchange was used previously to monitor the kinetics of RNase A unfolding, some peptide NH protons were found to show EX2 exchange (detected by base catalysis) in addition to the expected EX1 exchange, whose rate is limited by the kinetic unfolding process. In earlier work, two groups showed independently that a restricted two-process model successfully fits published hydrogen exchange rates of native RNase A in the range 0–0.7 M guanidinium chloride. We find that this model predicts properties that are very different from the observed properties of the EX2 exchange reactions of RNase A in conditions where guanidine-induced unfolding takes place. The model predicts that EX2 exchange should be too fast to measure by the technique used, whereas it is readily measurable. Possible explanations for the contradiction are considered here, and we show that removing the restriction from the earlier two-process model is sufficient to resolve the contradiction; instead of specifying that exchange caused by global unfolding occurs by the EX2 mechanism, we allow it to occur by the general mechanism, which includes both the EX1 and EX2 cases. It is logical to remove this restriction because global unfolding of RNase A is known to give rise to EX1 exchange in these unfolding conditions. Resolving the contradiction makes it possible to determine whether populated unfolding intermediates contribute to the EX2 exchange, and this question is considered elsewhere. The results and simulations indicate that moderate or high denaturant concentrations readily give rise to EX1 exchange in native proteins. Earlier studies showed that hydrogen exchange in native proteins typically occurs by the EX2 mechanism but that high temperatures or pH values above 7 may give rise to EX1 exchange. High denaturant concentrations should be added to the list of variables likely to cause EX1 exchange.**

To test for partially unfolded intermediates with some hydrogen bonds broken, the kinetic unfolding process of RNase A was monitored by NMR hydrogen exchange (H exchange) (1). In these conditions [4.5 M guanidinium chloride (GdmCl), 10°C, pH 8.0 or 9.0], H exchange is expected to follow the EX1 mechanism, in which the rate of unfolding limits the rate of H exchange. All the NH protons that exchange solely by the EX1 mechanism (42 of the 49 measured at pH 8.0) do so with the same rate constant. The rate of the unfolding step monitored by EX1 exchange is somewhat faster than the unfolding rate monitored by CD, but the difference is expected (1) because unfolding monitored by H exchange is not reversible, unlike unfolding monitored by optical probes, and because kinetic coupling occurs between unfolding and proline isomerization after unfolding. Thus, EX1 exchange is caused by the rate-limiting step in unfolding, and, if an unfolding intermediate (I) is formed, it must meet one of two conditions. (*i*) I occurs directly after the rate-limiting step in unfolding. Two or more steps may be involved in producing H exchange, but exchange occurs in a single kinetic phase without a measurable lag. (*ii*) I is in rapid equilibrium with N. Such an intermediate would equilibrate rapidly with the native protein at the start of the kinetic unfolding process, and it would be detected by EX2 exchange: see discussion of rapidly formed unfolding intermediates in ref. 2.

The terms EX1 and EX2 (3–5) refer to the two limiting cases of the general mechanism for exchange in proteins, in which the major conformation is exchange resistant and equilibrates with minor conformational states in which one or more NH protons are exchange susceptible. EX2 is the limiting case in which equilibration is rapid compared to the exchange step and, as a consequence, the observed exchange rate is base catalyzed, as is the exchange step. EX1 is the limiting case in which equilibration is slow compared to the exchange step. EX1 exchange is not base catalyzed, and the observed exchange rate gives the rate of unfolding or of local opening.

In the unfolding experiments, the exchange of several peptide NH protons was found to be dominated by a faster EX2 component, indicating the presence of a rapid $N \rightleftharpoons I$ equilibrium (1). This rapid EX2 exchange might result either from small fluctuations in the native structure, which is a commonly observed mechanism of EX2 exchange in native proteins (6, 7), or from a true unfolding intermediate. A critical distinction between exchange from a true unfolding intermediate and small fluctuations of the native state is the amount of surface area exposed in each process (8). The change in solvent-exposed surface area is believed to be measured directly by, and proportional to, m, the dependence of free energy on denaturant concentration. Bai, Englander, and coworkers (2) found recently that EX2 exchange rates of NH protons in cytochrome *c* are associated with events of both small and large m. Their results focus attention on the nature of the EX2 exchange reactions of RNase A in unfolding conditions.

The EX2 exchange reactions of RNase A measured as a function of GdmCl concentration in subdenaturing conditions (8) have been successfully described by a two-process model for exchange (6, 7). This model attributes EX2 exchange in native proteins to just two processes: small conformational fluctuations (process 1) and global unfolding (process 2). Exchange is described by an equation whose parameters are directly measurable. Earlier studies of H exchange in proteins have also been interpreted in terms of these two processes (9, 10). The term "two-process model" is used here to refer to the mathematical development of this model (6, 7).

When we attempted to interpret the EX2 exchange reactions of RNase A at the start of the kinetic unfolding process (1, 11), we encountered the following problem. Their properties are quite different from those predicted by the earlier two-process model for EX2 exchange (6, 7). The model predicts that, at denaturant concentrations beyond the midpoint of the unfold-

The publication costs of this article were defrayed in part by page charge payment. This article must therefore be hereby marked "*advertisement*" in accordance with 18 U.S.C. §1734 solely to indicate this fact.

Abbreviation: Gdm, guanidinium cation.

ing transition, EX2 exchange should occur at the fully solvent-exposed rates, equal to the exchange rates in model peptides. These exchange rates are too fast to measure by the technique used in the RNase A unfolding experiments, so that no EX2 exchange should have been measured if this prediction of the two-process model were correct.

There are at least three possible explanations for the differences between the predicted and observed exchange behavior. (*i*) The earlier two-process model applies to the EX2 exchange reactions of native proteins in conditions where the native protein is stable, whereas the results obtained in the RNase A unfolding experiments refer to the transient exchange behavior of the native protein at the start of unfolding. (*ii*) The earlier two-process model considers exchange by only two processes, global unfolding and small fluctuations: exchange that occurs from partly unfolded intermediate species is excluded. Partly unfolded intermediates that are formed rapidly at the start of the unfolding process might be well populated. (*iii*) The earlier two-process model restricts all exchange to the EX2 mechanism, but global unfolding in the RNase A unfolding experiments is known to result in EX1 exchange. This might affect the predicted properties of the EX2 exchange reactions even though they occur by small fluctuations and not by global unfolding.

We show here that the third explanation is correct and that it is sufficient to explain the entire contradiction. We also point out that the general two-process model used here may be useful in other exchange studies, because the effects noted here can occur in a wide range of conditions.

SIMULATION OF EXCHANGE KINETICS

The exchange kinetics were simulated by using the following two-process model. The kinetics simulation program KINSIM of Frieden and coworkers (12) was used.

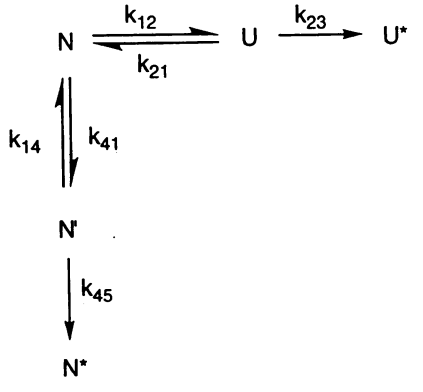

[1]

The model is written for a particular peptide NH proton (*i*); the subscript *i* is omitted. Process 1, leading to N′, occurs by small conformational fluctuations; the native protein N is exchange resistant, N′ is an exchange-susceptible, native-like form, and the exchanged species is N*. N′ is in rapid equilibrium with N, and explicit values for the rate constants k_{14}, k_{41} are not needed. N′ can be either on or off the pathway leading to U; the results do not distinguish between these two cases. Process 2 is global unfolding; U is the unfolded form and the exchanged species is U*. The exchange steps N′ → N* and U → U* are written as being irreversible because H → ^{2}H exchange takes place in $^2H_20$, or ^{2}H → H exchange takes in H_20. The rate constants for the two exchange steps are both assumed to be given by

$$k_{23} = k_{45} = k_b[OH^-], \quad [2]$$

where k_b is the rate constant for base-catalyzed exchange, which depends on sequence (i.e., on the two residues on either side of the peptide bond). Values of k_b are available from studies of H exchange in peptides; revised values were given recently (13). In $^2H_20$, $[OH^-]$ in Eq. **2** should be replaced by $[O^2H^-]$ (14). Eq. **2** applies above pH 4, where acid catalysis is not significant (13, 14).

In finding the correct values of k_{12} and k_{21} to use in Eq. **1**, account must be taken of the fact that the refolding kinetics of RNase A are complex; this has been known for a long time (15, 16). Complex refolding kinetics are the result both of proline isomerization after unfolding (17, 18) and of the formation of folding intermediates (19–22). In H-exchange experiments with native proteins, transient unfolding is followed rapidly by refolding, and the refolding rate constant k_{21} used in Eq. **1** refers to the fast-folding species with native prolyl isomers. Recent work (22, 23) has shown that this species of RNase A undergoes proline isomerization after unfolding more rapidly than was realized earlier and also that it refolds much more rapidly than realized earlier. Other recent work (24, 25) has found kinetic coupling between unfolding and proline isomerization in conditions (pH 6.0, 10°C, GdmCl-induced unfolding) similar to the ones discussed here. When kinetic coupling occurs, the unfolding kinetics become complex (24, 25) like the refolding kinetics. If, however, the unfolding rate constant k_{12} is measured by H exchange, then kinetic complexity does not affect the measured value of k_{12} because H exchange is irreversible (1).

RESULTS

Simulation of the H-Exchange Kinetics of RNase A in Two Conditions. Fig. 1 shows the H-exchange kinetics of native RNase A (8) in subdenaturing conditions, 0–0.7 M GdmCl, pH* 5.5, 34°C (pH* refers to the glass electrode reading in $^2H_20$, uncorrected for the isotope effect), and the interpretation of these results by the earlier two-process model (6); the figure has been reprinted from ref. 6. These results were also interpreted independently by others (7), using basically the same restricted two-process model. This two-process model assumes that a typical NH proton undergoes EX2 exchange at 0 M GdmCl by small fluctuations; the EX2 exchange rate does

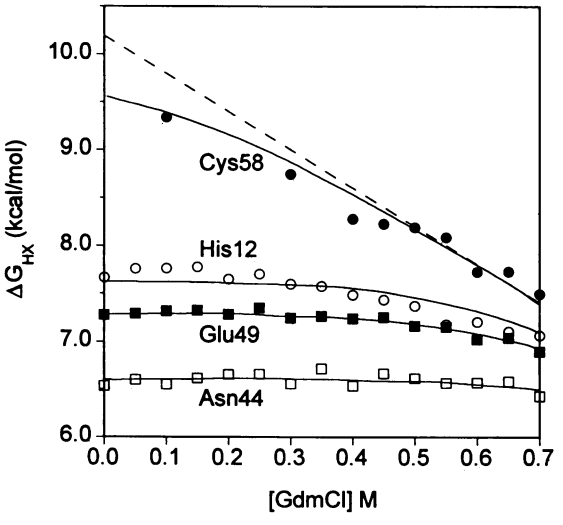

FIG. 1. H exchange rates of peptide NH protons in native RNase A (8), measured as a function of GdmCl molarity from 0 to 0.7 M, at pH* 5.5, 34°C, and interpreted by the restricted two-process model (6). $\Delta G^* = RT\ln P$, where P is the protection factor (see Eq. **6**) for EX2 exchange. Horizontal lines indicate exchange via small conformational fluctuations at 0 M GdmCl. Dashed line is predicted line for EX2 exchange via global unfolding. (Redrawn from ref. 6.)

not change significantly with increasing molarity of GdmCl until it is affected by global unfolding, whose rate depends strongly on GdmCl molarity. The horizontal exchange curves (Fig. 1) of all peptide NH protons intersect the diagonal exchange line for global unfolding before the midpoint of the unfolding transition zone, where $\Delta G°$ for global unfolding is 0.

Consequently, the earlier two-process model makes the following two predictions about EX2 exchange in the unfolding experiments of Kiefhaber and Baldwin (1): (*i*) EX2 exchange should occur only by global unfolding beyond C_m, the midpoint of the unfolding transition, and (*ii*) the protection factors of all peptide NH protons should equal unity beyond C_m. Both predictions are clearly contradicted by the data.

Fig. 2 shows the same data as Fig. 1, now interpreted by the general two-process model. The ordinate displays the reciprocal of the observed rate of H exchange, $1/k_{obs}$, rather than the derived quantity ΔG^*, which has no meaning if H exchange occurs by the EX1 mechanism. In the simulations of exchange shown in Fig. 1, the assumption is made that ΔG^* for exchange by global unfolding is equal to $\Delta G°$, the change in Gibbs energy for global unfolding measured by calorimetry or by optical probes. Thus, the dependence of ΔG^* on GdmCl molarity should be given by m_{12}, the coefficient relating $\Delta G°$ to molarity of GdmCl.

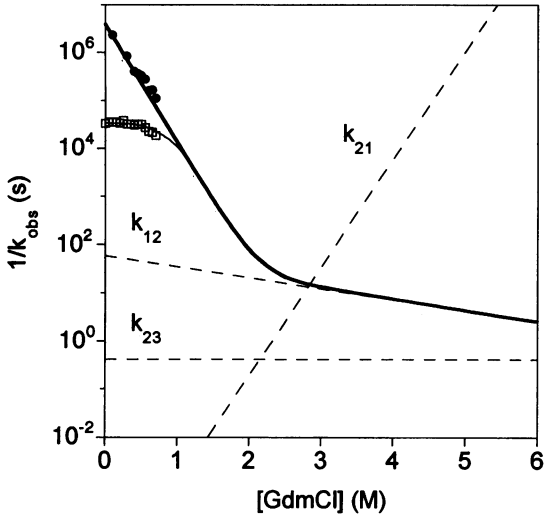

FIG. 2. Fitting the exchange data for RNase A shown in Fig. 1 by the general two-process model. A transition from EX2 to EX1 exchange is predicted to occur near 2.2 M GdmCl. Ordinate is the reciprocal of the exchange rate k_{obs}, instead of ΔG^* used in Fig. 1, because the derived quantity ΔG^* is appropriate only when exchange occurs by the EX2 mechanism. Boldface curve simulates exchange by global unfolding. Solid thin curve simulates exchange for peptide NH protons Cys-58 (●) and Glu-49 (□). Values used for ΔG^* (0) are those reported in ref. 8 adjusted to reflect the recently revised values of k_{23} (13) and are as follows (in kcal·mol^{-1}): Cys-58, 9.5; Glu-49, 6.7. The dependence of k_{12} on GdmCl concentration ($m^{\ddagger}_{12}$) was determined from unfolding experiments carried out at pH 6, 10°C (25). Values of k_{12} at 34°C are estimated to be 20-fold higher than those measured at 10°C (26): $m^{\ddagger}_{12}$ is assumed to be temperature independent. Global unfolding parameters $\Delta G°(0)$ and m_{12} (8.4 kcal·mol^{-1} and 3.5 kcal·mol^{-1} M^{-1} respectively) were determined from a linear least-squares fit of calorimetric data collected at several different GdmCl concentrations (27). A correction factor of 1.4 kcal·mol^{-1} is added to $\Delta G°(0)$ to account for the fact that H exchange takes place exclusively from the unfolded form with native proline isomers (6, 24). This correction results in a $\Delta G^*(0)$ value for global unfolding of 9.8 kcal·mol^{-1}. The dependence of k_{21} on GdmCl ($m^{\ddagger}_{21}$) was deduced from the relationship $m_{12} = m^{\ddagger}_{12} - m^{\dagger}_{21}$. To obtain k_{23}, the chemical exchange rates of all NH protons in RNase A were calculated at pH* 5.5, 34°C and averaged. Exchange kinetics were simulated using the program KINSIM (12).

$$\Delta G°_{12} = \Delta G°_{12}(0) - m_{12}\,\mathrm{M} \quad [3]$$

In fact, the *m* values shown by the two most slowly exchanging NH protons, Cys-58 and Cys-84, are close to the value of m_{12} measured in separate unfolding experiments.

In contrast to the continuous EX2 exchange behavior simulated in Fig. 1, a transition from EX2 exchange to EX1 exchange is predicted in Fig. 2 for exchange via global unfolding. This transition should occur when the exchange rate k_{23} becomes faster than the refolding rate k_{21} and the unfolding rate k_{12} (3, 4). When EX1 exchange occurs, the dependence of $\ln k_{obs}$ on molarity of GdmCl is governed by $m^{\ddagger}_{12}$, the *m* value for the unfolding rate constant, rather than by the equilibrium parameter m_{12}. Provided the unfolding reaction follows the two-state model (if there are no folding intermediates, and the transition state is independent of GdmCl molarity), then the dependences of the unfolding and refolding rate constants on GdmCl molarity are given (28):

$$-RT\ln k_{12} = -RT\ln k_{12}(0) - m^{\ddagger}12\,\mathrm{M} \quad [4a]$$

$$-RT\ln k_{21} = -RT\ln k_{21}(0) - m^{\ddagger}21\,\mathrm{M} \quad [4b]$$

Thus, the predicted transition from EX2 to EX1 exchange in Fig. 2 is accompanied by a change in slope of $\ln k_{obs}$ versus GdmCl M from (m_{12}/RT) to $(m^{\ddagger}_{12}/RT)$.

The parameters are not known accurately that are needed to predict the molar value of GdmCl at which a transition from EX2 exchange to EX1 exchange takes place, for the following reasons. The correct values of k_{12}, k_{21}, $m^{\ddagger}_{12}$ and $m^{\ddagger}_{21}$ needed in the simulation of exchange kinetics must satisfy a strict two-state mechanism in the conditions studied, and consequently m_{12} must equal $m^{\ddagger}_{12} - m^{\ddagger}_{21}$. Available data (22, 25) cast doubt on whether this basic requirement is satisfied by RNase A in the conditions considered here. A second, more general, problem is that the rate of the exchange step in the protein may not be given accurately by exchange data from peptides, as assumed in Eq. **2**. There may be hindered access of OH^- ion to the site of exchange in the protein. This was given as a possible explanation (8) when ΔG^* for RNase A exchange via global unfolding was found to be larger than $\Delta G°$ measured by optical probes. Part of the difference between ΔG^* and $\Delta G°$ is explained for RNase A by the effect of proline isomerization after unfolding (6, 24, 25), but whether peptide exchange data can be used to model quantitatively the rate of the exchange step in proteins still needs careful study.

The basic point made in Fig. 2 is that a transition from the EX2 mechanism to the EX1 mechanism for exchange via global unfolding is predicted to occur as the GdmCl concentration increases. The molar value of GdmCl at which the transition should occur cannot yet be predicted accurately.

Fig. 3 shows the simulated exchange kinetics of RNase A at pH 8.0, 10°C, in an unfolding experiment made at 4.5 M GdmCl (1). The simulation predicts a transition for exchange via global unfolding from the EX2 mechanism to the EX1 mechanism at ≈2 M GdmCl. Global unfolding was found experimentally to cause EX1 exchange not only at 4.5 M GdmCl (1) but also at 2.5 M GdmCl, before the onset of the unfolding transition (T.K. and R.L.B., unpublished experiments). In contrast to the two-process model used in Fig. 1, this simulation predicts that EX2 exchange via small fluctuations will still take place beyond the midpoint of the unfolding transition zone. The reason why this behavior is predicted to occur at pH 8.0, 10°C, but not at pH* 5.5, 34°C, is considered in the *Discussion*. Although the simulations of exchange kinetics shown in Figs. 2 and 3 are discussed in terms of limiting cases (EX1 and EX2 behavior), the simulations themselves are made using the general mechanism, which includes EX1 and EX2 exchange as limiting cases.

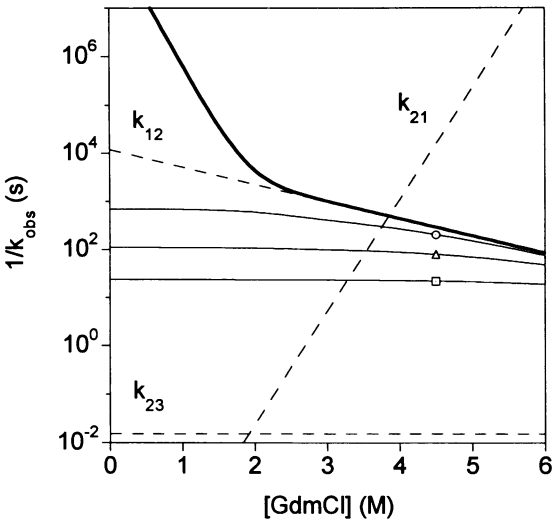

FIG. 3. Use of the general two-process model to interpret the exchange kinetics of RNase A measured in unfolding conditions (pH 8, 10°C, 4.5 GdmCl). The predicted exchange behavior over the entire range 0–6 M GdmCl is shown. Note that EX2 exchange via small fluctuations is predicted to occur at GdmCl concentrations beyond the unfolding transition zone. Solid line is predicted exchange via global unfolding. Thin solid lines simulate exchange for peptide NH protons Met-30 (○), Arg-33 (△), and Cys-65 (□); the corresponding values of $\Delta G^*(0)$ are (in kcal·mol^{-1}) 5.7, 5.0, and 4.4, respectively. Value of $m^{\ddagger}_{12}$ is taken from data at 10°C, pH 8 (T.K., unpublished results) and the unfolding rate k_{12} at 4.5 GdmCl is 3.4×10^{-3} s^{-1} from H exchange data (1); with this procedure, k_{12} is not affected by proline isomerization after unfolding. From the midpoint of the equilibrium unfolding transition (3.57 M GdmCl, T.K., unpublished results) and the value of $m^{\ddagger}_{21}$ (obtained as in Fig. 2), one can calculate the rate of refolding starting from the equilibrium mixture of unfolded species with different proline isomers. This rate, divided by k_{12} at 0 M GdmCl and adjusted for the proline effect (see legend to Fig. 2), yields a value of $\Delta G^*(0)$ for global unfolding of 13.4 kcal·mol^{-1}. The midpoint of the unfolding transition as monitored by hydrogen exchange (i.e., where $k_{12} = k_{21}$) is displaced by = +0.5 M GdmCl relative to the equilibrium unfolding midpoint.

Observed Protection Factors for EX2 Exchange at pH 8.0, 10°C. To find the process that gives rise to EX2 exchange in the unfolding experiment at pH 8.0, 4.5 M GdmCl, 10°C, it is necessary to determine the protection factors. This can be done using the relations

$$k_{obs} = k_{EX1} + k_{EX2} \quad [5]$$

$$P = k_b[OH^-]/k_{EX2}. \quad [6]$$

Relation **5** applies because the exchange rates of independent processes are additive, and this is true of the two processes in Eq. **1**. Relation **6** gives the protection factor P, which is defined as the exchange rate in a fully solvent-exposed NH proton divided by the EX2 exchange rate of this proton in the protein. Because EX1 exchange occurs by global unfolding, k_{EX1} has the same value for all NH protons and the mean value of k_{EX1} (3.4×10^{-3} s^{-1} at pH 8.0) can be used to find k_{EX2} from k_{obs}. The values of k_{obs} for all protons, at both pH 8.0 and pH 9.0, are given in Table 1.

Two criteria are used to identify protons that show significant EX2 exchange: (*i*) $k_{obs} > (\langle k_{EX1} \rangle + 3\sigma)$, where $\langle k_{EX1} \rangle$ is the mean value of k_{EX1} and where σ is the average standard deviation of k_{EX1} measured from individual exchange curves; (*ii*) the proton must show EX2 exchange at pH 9.0 if it shows EX2 exchange at pH 8.0. The second criterion follows because EX2 exchange is base catalyzed and should be 10 times faster at pH 9.0 than at pH 8.0. By these two criteria, 7 protons show EX2 exchange at both pH 8.0 and pH 9.0 (Met-30, Arg-33, Asn-34, Val-43, Ser-59, Cys-65, and Val-124), and 8 more protons show detectable EX2 exchange only at pH 9.0 (Glu-9, Lys-31, Asp-53, Gln-60, Lys-61, Glu-86, Tyr-97, and Cys-110). Some other peptide NH protons show observable exchange at pH 8.0 but their values of k_{obs} are too large to measure.

Excluding Val-124, whose protection factor is anomalously low ($P = 20$) because Val-124 is C-terminal and has an unusual value of k_b, the smallest protection factor is shown by Cys-65 ($P = 2500$). The largest protection factor that still allows measurement of detectable EX2 exchange is about $P = 1 \times 10^5$, shown by Glu-86 and Cys-110.

DISCUSSION

EX2 Exchange at pH 8.0 and pH 9.0, 4.5 M GdmCl, 10°C, Occurs by Small Fluctuations. This conclusion rests on three observations. (*i*) The observed protection factors for EX2 exchange in unfolding conditions are diverse and span a broad range, as expected for exchange via small fluctuations. This result is opposite to the expectation for exchange via global unfolding. Excluding Val-124, the range of P is from 2.5×10^3 to 1×10^5. (*ii*) EX2 exchange via small fluctuations is predicted to occur in these unfolding conditions when the general two-process model is used (see Fig. 3). (*iii*) The protection factors for EX2 exchange at pH* 5.5, 34°C, 0 M GdmCl, and at pH 8.0, 10°C, 4.5 M GdmCl, are closely correlated with each other (Fig. 4). Thus, EX2 exchange occurs by the same process in both sets of conditions, and it has been shown earlier (6, 7) that these NH protons undergo EX2 exchange via small fluctuations at pH* 5.5, 34°C.

EX2 Exchange Via Small Fluctuations Is Predicted to Occur Beyond C_m at pH 8.0, 10°C, but Not at pH* 5.5, 34°C. Although a transition from EX2 exchange to EX1 exchange is predicted to occur before C_m in both sets of conditions, EX2 exchange via small fluctuations is predicted to occur beyond C_m only at pH 8.0, 10°C. The reason is as follows. Exchange occurs by the fastest pathway and so EX2 exchange via small fluctuations can occur if it is faster than EX1 exchange via global unfolding: see Eq. **1**. At pH 8.0, 10°C, the rate of EX1 exchange via global unfolding (3.4×10^{-3} s^{-1} at 4.5 M GdmCl) is much slower than at pH* 5.5, 34°C ($k_{EX1} > 10^{-1}$ s^{-1} at C_m; Fig. 2). The EX2 rate is base-catalyzed and, because the base concentration ([OH^-] or [O^2H^-]) is much higher at pH 8.0 than at pH* 5.5, this factor also favors EX2 exchange via small fluctuations at pH 8.0. The protection factors of these EX2 reactions are not greatly different at pH* 5.5, 34°C, and at pH 8.0, 10°C (Fig. 4), and so the base concentration is the main factor that determines the EX2 exchange rate: see Eq. **6**. Both the relative rates of global unfolding and of EX2 exchange contribute to the explanation of this effect.

Induction of EX1 Exchange by GdmCl. In two different sets of conditions, the simulations predict that a transition from EX2 to EX1 exchange should occur for exchange via global unfolding as the GdmCl concentration increases (Figs. 2 and 3). This transition is caused primarily by the rapid decrease in the refolding rate with increasing GdmCl concentration. [The effect of GdmCl on k_b (32) has been neglected.] It is customary to assume that in conditions such as pH* 5.5, 34°C, only EX2 exchange will occur (6–8), but it is now clear that high denaturant concentrations may induce EX1 exchange. An experimental study (33) of the occurrence of EX1 exchange in bovine pancreatic trypsin inhibitor showed that it occurs only in exceptional conditions and in the most stable peptide NH protons. Conditions that increase the rate of the exchange step (k_{23}) or decrease the rate of refolding (k_{21}) can induce EX1 exchange. These include raising the pH (e.g., above pH 7) (33, 34) or raising the temperature (33, 35, 36), or, as we point out here, raising the denaturant concentration.

Structural Locations of Classes of Peptide NH Protons with Various EX2 Rates. Fig. 5 shows the locations in the RNase A

Table 1. Relaxation times for H exchange during unfolding

Amide proton	Secondary structure	H-bond acceptor†	$1/k_{obs}$, s	
			pH 8.0	pH 9.0
E2	—	?	<5	<10
A6	Helix 1	?	<5	<10
K7	Helix 1	T3 O	<5	<10
E9	Helix 1	A5 O	309 ± 46	142 ± 16
R10	Helix 1	A6 O	356 ± 50	216 ± 19
Q11	Helix 1	K7 O	290 ± 40	177 ± 17
H12	Helix 1	F8 O	291 ± 35	206 ± 22
M13	Helix 1	E9 O	266 ± 28	172 ± 6
D14	Loop	V47 O	228 ± 19	175 ± 25
C26	Helix 2	?	<5	<10
N27	Helix 2	N24 O	<5	<10
Q28	Helix 2	?	<5	<10
M29	Helix 2	Y25 O	279 ± 35	202 ± 11
M30	Helix 2	C26 O	204 ± 50	138 ± 24
K31	Helix 2	N27 O	249 ± 19	78 ± 7
R33	Helix 2	M29 O	80 ± 40	<10
N34	Helix 2	K31 O	93 ± 40	<10
V43	β-Sheet 1	?	240 ± 20	157 ± 13
N44	β-Sheet 1	C84 O	278 ± 27	235 ± 16
F46	β-Sheet 1	T82 O	294 ± 35	248 ± 27
V47	β-Sheet 1	H12 O	258 ± 23	220 ± 16
H48	β-Sheet 1	S80 O	269 ± 40	236 ± 11
E49	Loop	?	244 ± 26	217 ± 39
D53	Helix 3	?	309 ± 80	85 ± 30
V54	Helix 3	L51 O	293 ± 24	229 ± 9
Q55	Helix 3	L51 O	340 ± 50	214 ± 38
A56	Helix 3	A52 O	304 ± 32	201 ± 11
V57	Helix 3	V54 O	292 ± 45	208 ± 33
C58	Helix 3	Q55 O	316 ± 45	245 ± 26
S59	Helix 3	A56 O	216 ± 15	22 ± 8
Q60	Helix 3	V57 O	257 ± 23	35 ± 7
K61	β-Sheet 2	Q74 O	276 ± 32	24 ± 8
V63	β-Sheet 2	C72 O	285 ± 17	232 ± 7
C65	Loop	Q69 O	22 ± 10	<10
C72	β-Sheet 2	V63 O	291 ± 27	220 ± 13
Y73	β-Sheet 2	V108 O	283 ± 35	222 ± 5
Q74	β-Sheet 2	K61 O	275 ± 25	212 ± 12
M79	β-Sheet 1	K104 O	247 ± 40	294 ± 60
I81	β-Sheet 1	A102 O	309 ± 20	227 ± 10
T82	β-Sheet 1	F46 O	287 ± 25	265 ± 28
D83	β-Sheet 1	T100 O	269 ± 23	185 ± 13
C84	β-Sheet 1	N44 O	292 ± 14	235 ± 13
R85	β-Sheet 1	K98 O	303 ± 26	210 ± 13
E86	β-Sheet 1	P42 O	285 ± 150	154 ± 24
Y97	Tertiary	N27 $O_{\delta}1$	264 ± 26	107 ± 20
K98	β-Sheet 1	R85 O	263 ± 20	359 ± 70
K104	β-Sheet 1	M79 O	284 ± 23	239 ± 25
I106	Tertiary	S75 O_{γ}	285 ± 20	218 ± 15
V108	β-Sheet 2	Y73 O	314 ± 30	224 ± 18
A109	β-Sheet 2	H119 O	269 ± 30	236 ± 8
C110	β-Sheet 2	N71 O	294 ± 41	75 ± 30
N113	β-Sheet 2	?	<5	<10
V116	β-Sheet 2	E111 O	273 ± 19	253 ± 25
V118	β-Sheet 2	A109 O	292 ± 24	230 ± 15
H119	β-Sheet 2	A109 O	295 ± 18	202 ± 6
V124	β-Sheet 2	H105 O	77 ± 18	<10

The unfolding experiments, in which H exchange is initiated simultaneously with unfolding, are made at pH 8.0 and pH 9.0, 10°C, in 4.5 M GdmCl (1). The deuterated native protein is diluted from ^2H_2O into H_2O containing concentrated GdmCl at the start of unfolding. At various times, exchange is quenched by dropping the pH to 4.0 and diluting the GdmCl so that refolding can occur. The extent of exchange of each peptide NH proton is then determined from a two-dimensional NMR spectrum (1).
†From refs. 29 and 30.

structure of 4 classes of NH protons with different EX2 exchange rates: (*i*) too slow to measure (chiefly protons inside helices 1 and 3 and in the β-sheet), (*ii*) measurable (protons at the ends of helices and β-strands, and inside helix 2), (*iii*) too fast to measure, but showing observable exchange (protons at the N-terminal end of helices 1 and 2, and in loops), and (*iv*)

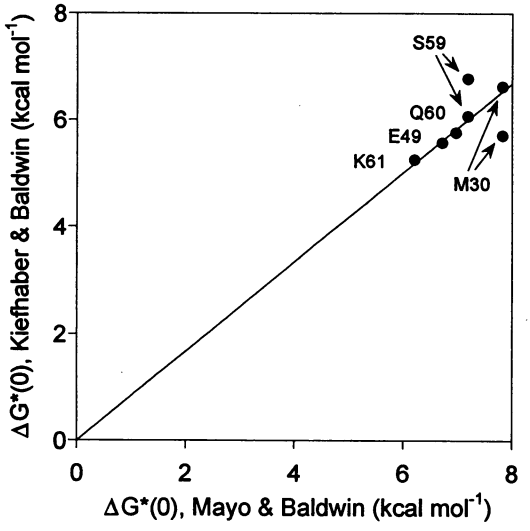

FIG. 4. Correlation of ΔG^* values at 0 M GdmCl for EX2 exchange via small fluctuations at pH* 5.5, 34°C (8) and at pH 8 and pH 9, 10°C (1). The latter data are based on experimental values measured at 4.5 M GdmCl (see Table 1) and the general two-process model has been used to estimate the values at 0 M GdmCl. Two values of ΔG^* at 10°C are shown for a few protons which give measurable EX2 exchange rates at both pH 8 and pH 9. The good correlation between $\Delta G^*(0)$ values measured in the two different experiments indicates that the same mechanism of EX2 exchange applies in both conditions.

too fast to observe (in loops). This pattern, obtained for RNase A at the start of unfolding, is similar to the pattern found in a pioneering study of pancreatic trypsin inhibitor in native conditions (37). The EX2 exchange rate gives the fraction of time that the peptide H bond is broken and the NH proton is exposed to solvent. Thus, these rates measure directly the structural loosening of the protein molecule. The diversity of EX2 rates provides a striking contrast to the constancy of the EX1 rates measured in the same unfolding conditions. The EX1 rates reflect a single catastrophic event, such as the entry of water into the hydrophobic cores, which converts the exchange-resistant native protein into an exchange-susceptible species, such as a molten globule.

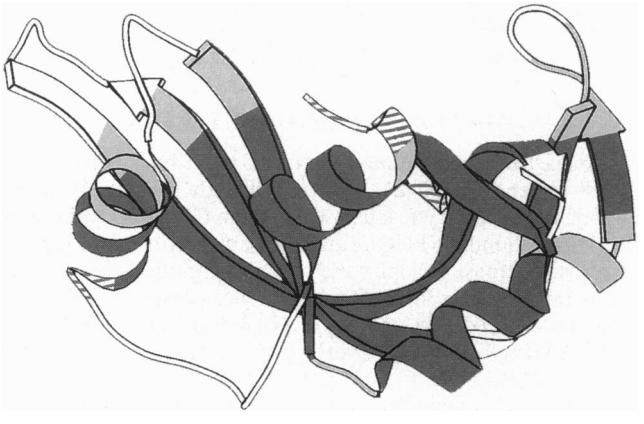

FIG. 5. Structural locations of different classes of peptide NH protons of RNase A in unfolding conditions, according to their EX2 exchange rates. Dark shading, too slow to measure; light shading, measurable; hatched, observable but too fast to measure accurately; open, too fast to observe exchange. The figure was drawn using MOLSCRIPT (31).

We thank Walter Englander for discussion, for permission to reproduce Fig. 1, and for a preprint of ref. 2. We also thank Jon Goldberg and Hong Qian for discussion. This work was supported by Grant GM 19988 to R.L.B. from the U.S. National Institutes of Health and by a grant to T.K. from the Schweizerische Nationalfonds. S.N.L. is a Fellow of the Damon Runyon–Walter Winchell Cancer Fund (DRG 1229).

1. Kiefhaber, T. & Baldwin, R. L. (1995) *Proc. Natl. Acad. Sci. USA* **92,** 2657–2661.
2. Bai, Y., Sosnick, T. R., Mayne, L. & Englander, S. W. (1995) *Science* **269,** 192–197.
3. Hvidt, A. & Nielsen, S. O. (1966) *Adv. Protein Chem.* **21,** 287–386.
4. Englander, S. W. & Kallenbach, N. (1984) *Q. Rev. Biophys.* **16,** 521–655.
5. Woodward, C., Simon, I. & Tüchsen, E. (1982) *Mol. Cell. Biochem.* **48,** 135–160.
6. Bai, Y., Milne, J. S., Mayne, L. & Englander, S. W. (1994) *Proteins Struct. Funct. Genet.* **20,** 4–14.
7. Qian, H., Mayo, S. L. & Morton, A. (1994) *Biochemistry* **33,** 8167–8171.
8. Mayo, S. L. & Baldwin, R. L. (1993) *Science* **262,** 873–876.
9. Rosenberg, A. & Chakravarti, K. (1968) *J. Biol. Chem.* **243,** 5193–5201.
10. Woodward, C. K. & Hilton, B. D. (1980) *Biophys. J.* **32,** 561–577.
11. Kiefhaber, T. & Baldwin, R. L. (1995) *Biophys. Chem.*, in press.
12. Barshop, A., Wrenn, R. F. & Frieden, C. (1983) *Anal. Biochem.* **130,** 134–145.
13. Bai, Y., Milne, J. S., Mayne, L. & Englander, S. W. (1993) *Proteins Struct. Funct. Genet.* **17,** 75–86.
14. Connelly, G. P., Bai, Y., Jeng, M.-F. & Englander, S. W. (1993) *Proteins Struct. Funct. Genet.* **17,** 87–92.
15. Garel, J. R. & Baldwin, R. L. (1973) *Proc. Natl. Acad. Sci. USA* **70,** 3347–3351.
16. Hagerman, P. J. & Baldwin, R. L. (1976) *Biochemistry* **15,** 1462–1472.
17. Brandt, J. F., Halvorson, H. R. & Brennan, M. (1975) *Biochemistry* **14,** 4953–4963.
18. Schmid, F. X. & Baldwin, R. L. (1978) *Proc. Natl. Acad. Sci. USA* **75,** 4764–4768.
19. Cook, K. H., Schmid, F. X. & Baldwin, R. L. (1979) *Proc. Natl. Acad. Sci. USA* **76,** 6157–6161.
20. Schmid, F. X. (1983) *Biochemistry* **22,** 4690–4696.
21. Udgaonkar, J. B. & Baldwin, R. L. (1995) *Biochemistry* **34,** 4088–4096.
22. Houry, W. A., Rothwarf, D. M. & Scheraga, H. A. (1995) *Nat. Struct. Biol.* **2,** 495–503.
23. Houry, W. A., Rothwarf, D. M. & Scheraga, H. A. (1994) *Biochemistry* **33,** 2516–2530.
24. Kiefhaber, T., Kohler, H.-H. & Schmid, F. X. (1992) *J. Mol. Biol.* **224,** 217–229.
25. Kiefhaber, T. & Schmid, F. X. (1992) *J. Mol. Biol.* **224,** 231–240.
26. Nall, B. T., Garel, J.-R. & Baldwin, R. L. (1978) *J. Mol. Biol.* **118,** 317–330.
27. Makhatadze, G. & Privalov, P. L. (1992) *J. Mol. Biol.* **226,** 491–505.
28. Chen, B.-L., Baase, W. A., Nicholson, H. & Schellman, J. A. (1992) *Biochemistry* **31,** 1464–1476.
29. Wlodawer, A., Svensson, L. A., Sjökun, L. & Gilliland, G. L. (1988) *Biochemistry* **27,** 2705–2717.
30. Santoro, J., Gonzalez, C., Bruix, M., Neira, J. L., Nieto, J. L., Hernanz, J. & Rico, M. (1993) *J. Mol. Biol.* **229,** 722–734.
31. Kraulis, J. (1991) *J. Appl. Crystallogr.* **24,** 946–950.
32. Loftus, D., Gbenle, G. O., Kim, P. S. & Baldwin, R. L. (1986) *Biochemistry* **25,** 1428–1436.
33. Roder, H., Wagner, G. & Wüthrich, K. (1985) *Biochemistry* **24,** 7396–7407.
34. Tanford, C. (1970) *Adv. Protein Chem.* **24,** 1–95.
35. Miranker, A., Robinson, C. V., Radford, S. E., Aplin, R. T. & Dobson, C. M. (1993) *Science* **262,** 896–900.
36. Swint-Kruse, L. & Robertson, A. D. (1995) *Biochemistry* **35,** 171–180.
37. Wagner, G. & Wüthrich, K. (1982) *J. Mol. Biol.* **160,** 343–361.